We are IntechOpen,
the world's leading publisher of
Open Access books
Built by scientists, for scientists

6,900
Open access books available

185,000
International authors and editors

200M
Downloads

154
Countries delivered to

Our authors are among the

TOP 1%
most cited scientists

12.2%
Contributors from top 500 universities

CLARIVATE ANALYTICS

BOOK CITATION INDEX

INDEXED

WEB OF SCIENCE™

Selection of our books indexed in the Book Citation Index
in Web of Science™ Core Collection (BKCI)

Interested in publishing with us?
Contact book.department@intechopen.com

Numbers displayed above are based on latest data collected.
For more information visit www.intechopen.com

Organic RFID Tags

Kris Myny[1,2,3], Soeren Steudel[1], Peter Vicca[1], Monique J. Beenhakkers[4],
Nick A.J.M. van Aerle[4], Gerwin H. Gelinck[5], Jan Genoe[1,2],
Wim Dehaene[1,3], and Paul Heremans[1,3]

[1]*IMEC vzw, Leuven,*
[2]*Katholieke Hogeschool Limburg, Diepenbeek,*
[3]*Katholieke Universiteit Leuven, Leuven,*
[4]*Polymer Vision, Eindhoven,*
[5]*TNO Science and Industry, Eindhoven,*
[1,2,3]*Belgium*
[4,5]*The Netherlands*

1. Introduction

In this chapter, we investigate the potential of organic RFID tags as a product label. The primary market for organic RFID tags could be barcode replacement, i.e. tags that generate a fixed code sequence when powered by an RF field. We infer this from the current state of the art of the technology: code generators that generate code sequences up to 128 bit are possible in organic electronics (Myny et al., 2009) and chips comprising 414 organic-based thin-film transistors (OTFTs) can today be integrated into fully functional organic RFID tags with HF communication frequency of 13.56 MHz (Myny et al., 2009). More complex RFID embodiments that comprise e.g. encryption, re-programmable code stored in a non-volatile memory, and true bi-directional communication with a reader are beyond the current state-of-the-art of organic electronics, but can be envisioned in a more distant future.

With 64 bit of data, that is read out in 10 to 20 ms, a realistic electronic tag for item-level identification can carry and read out the standard Electronic Product Code (EPC, http://www.epcglobalinc.org/). We have shown that these requirements to the complexity of the chip and the clock frequency can be obtained.

We further assume that product identification tags should preferably be passive tags, that do not include a battery, since the integration of a battery would considerably increase the cost of a tag. Passive tags are powered by the electromagnetic field of the reader, also called interrogator. To power passive organic RFID tags, high-quality organic rectifiers are needed and these need to be very carefully designed. We have been able to obtain sufficient DC voltage to power organic code generators by organic rectifiers, using reader fields that comply with the standards imposed by the safety rules concerning electromagnetic radiation.

Several research groups have published research results on organic RFID systems. In 2007, Cantatore et al. published a capacitively-coupled RFID system where a 64-bit code was read out at a base carrier frequency of 125 kHz (Cantatore et al., 2007). The 64-bit code generator

was fully functional at a 30 V supply voltage. In that pioneering work, lower bit generators (up to 6 bit) could be read out using a base carrier frequency of 13.56 MHz by a capacitive antenna. Ullmann et al. demonstrated a 64-bit tag working at a bit rate exceeding 100 b/s, readout by inductive coupling at a base carrier frequency of 13.56 MHz (Ullmann et al., 2007). We review in this chapter recent advances in both the digital transponder chip and the analog front-end of organic RFID tags, and demonstrate that organic electronics can result in a tag with a realistic code size, bit rate and reading distance at a reasonable and allowed field strength (Myny et al., 2008; Myny et al., 2009). We also demonstrate significant increases in complexity of RFID transponder chips where the data have been Manchester encoded and a basic anti-collision protocol has been added that will allow the readout of multiple organic RFID tags in the field of a single reader at once (Myny et al., 2009).

The different sections in this chapter discuss the following building blocks of an organic RFID tag: the antenna coil, the HF-capacitor, the rectifier and the 64-bit transponder chip with integrated load modulator. The coil and HF-capacitor match the resonance frequency of 13.56 MHz, and absorb energy transmitted by the reader and power the organic rectifier with an AC voltage at 13.56 MHz. The rectifier generates the DC supply voltage for the organic transponder chip, which drives the modulation transistor between the on- and off-state with the code sequence.

2. Components of the organic RFID tag

The basic schematic of the organic RFID tag presented here is depicted in Fig. 1. The organic RFID tag consists of 4 different modules: the antenna coil, the HF-capacitor, the rectifier and the transponder chip with an integrated load modulator. The coil and the HF-capacitor form an LC tank resonating at the HF resonance frequency of 13.56 MHz, which energizes the organic rectifier with an AC voltage at 13.56 MHz. The rectifier generates the DC supply voltage for the 64-bit organic transponder chip, which drives the modulation transistor between the on- and off-state with a 64-bit code sequence. Load modulation can be obtained in two different modes, depending on the position of the load modulation transistor in the RFID circuit, shown in Fig. 1. AC load modulation, whereby the modulation transistor is placed in front of the rectifier, sets demanding requirements to the OTFT, since it has to be able to operate at HF frequency. This is not obvious, as a consequence of the limited charge carrier mobility of the OTFT, $0.1 - 1$ cm^2/Vs for pentacene as organic semiconductor. Therefore, load modulation at the output of the rectifier (DC load modulation) is preferred in organic RFID tags. In latter mode, the OTFT does not require to operate at HF frequency. The organic RFID tags in this chapter operate in DC load modulation mode. Nevertheless, organic RFID tags operating in AC load modulation mode have also been achieved (Myny et al., 2009).

2.1 Technology

In this part we describe the technology used to create high-performance organic RFID tags (Myny et al., 2009). As mentioned earlier, the tags are composed of four flexible foils, with the following components: an inductor coil, a capacitor, a rectifier and a transponder. The coil is made from etched copper on foil, and was manufactured by Hueck Folien GmbH.

The HF-capacitor consists of a metal-insulator-metal stack (MIM stack), processed on a 200-μm thick flexible polyethylene naphthalate (PEN) foil (Teonex Q65A, Dupont Teijin Films). The insulator material used for the capacitor is Parylene diX SR.
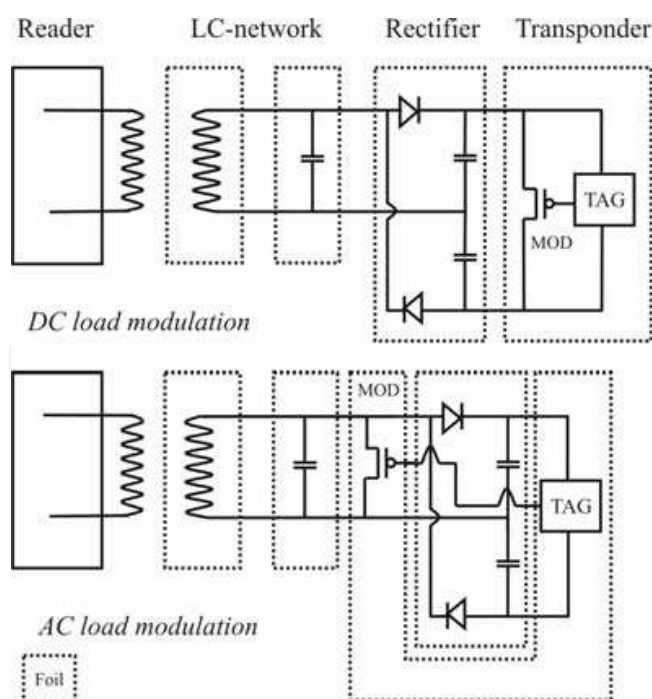
Fig. 1. Inductively-coupled organic RFID tags using DC (top pane) and AC (bottom panel) load modulation.

The rectifier comprises two vertical Schottky diodes, and two capacitors in a so-called double half-wave configuration. The schematic of the rectifier is shown in Fig. 9, and a photograph of the rectifier is depicted in Fig. 2. The substrate for manufacturing the rectifiers is a 200 μm thick, flexible 150 mm PEN foil, on which first a metal-insulator-metal (MIM) stack is processed for the capacitors in the circuit. The metal layers are 30 nm of gold (Au) and the insulator is Parylene diX SR, with a relative dielectric constant of ε_r of 3 and a thickness of 400 nm. Conventional photolithography is used to define the capacitors in the MIM stack. The top Au layer of the MIM stack is used as anode for the vertical diode. A 350 nm pentacene layer, the organic semiconductor, is evaporated through a shadowmask by HV-deposition. Last, an aluminum (Al) cathode is evaporated through a second shadowmask.

The organic 64-bit transponder chip is made on a 25 μm thin plastic substrate using organic bottom-gate thin-film transistors. The organic electronics technology that is used, was developed by Polymer Vision for commercialization in rollable active matrix displays and is described elsewhere (Huitema et al., 2003; Gelinck et al., 2004). The insulator layers and the semiconductor layer are organic materials processed from solution. The transistors, with a typical channel length of 5 μm, exhibit an average saturation mobility of 0.15 cm^2/Vs. A micrograph picture of the 64-bit transponder chip and the 6" wafer is depicted in Fig. 2.

2.2 The RFID measurement setup
The complete tag is realized by properly interconnecting the contacts of the four foils, which we achieved in an experimental set-up where we plug the individual foils into sockets as shown in Fig. 3. Alternatively, we have also achieved tags by lamination of the foils, whereby electrically conductive glue is used to interconnect the different contacts of the individual foils.
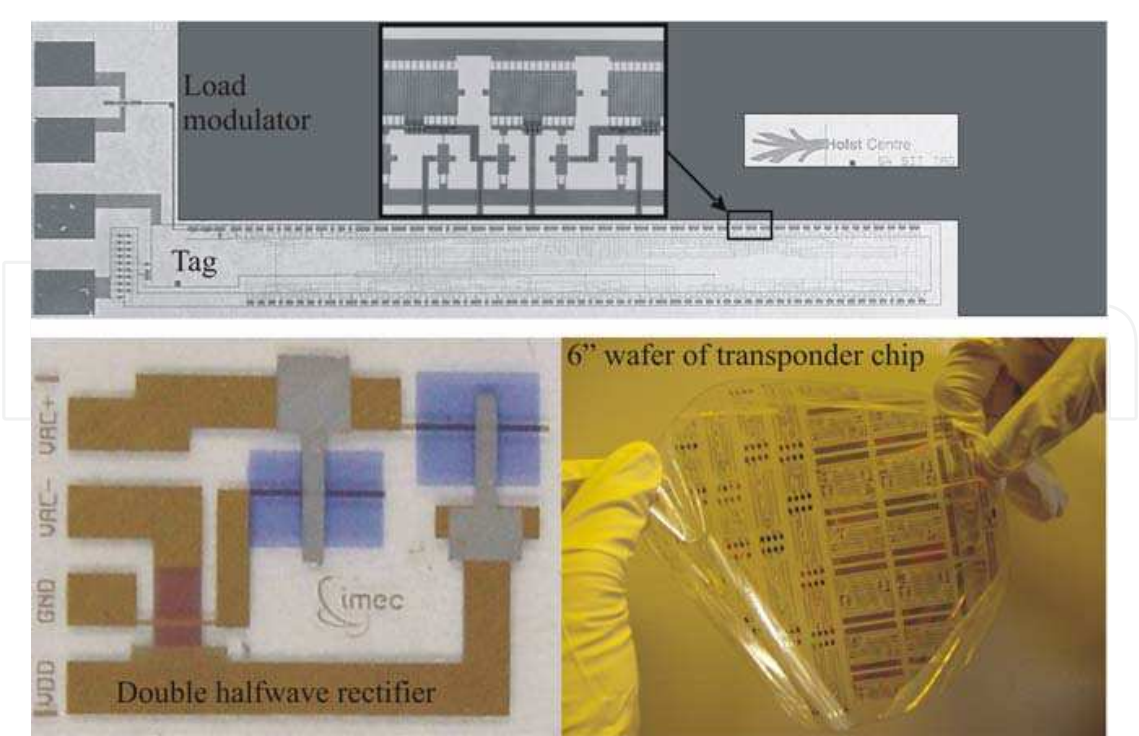
Fig. 2. Pictures of the transponder foil and the load modulator foil (top), the double half-wave rectifier foil (bottom left) and the 6" wafer full of transponder chips (bottom right).

The reader setup conforms to the ECMA-356 standard for "RF Interface Test Methods". It comprises a field generating antenna and two parallel sense coils (Fig. 3), which are matched to cancel the emitted field. By this method, only the signal sent by the RFID tag is read out at the reader side. The detected signal is then demodulated by a simple envelope detector (inset Fig. 12), being a diode followed by a capacitor and a resistor, and shown on an oscilloscope.
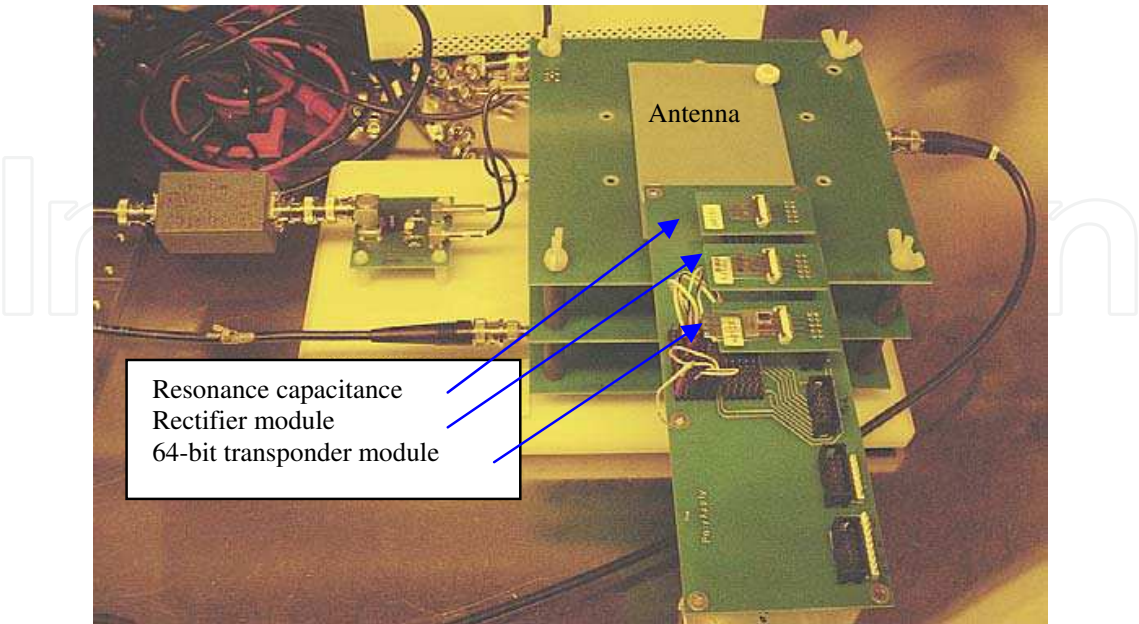

Fig. 3. Overview of the reader and RFID tag measurement setup. Foils are placed in sockets to ease manipulation.

3. Organic transponder chip

3.1 Design issues for the organic RFID transponder chip

In this part, we will discuss challenges in designing large, robust circuitry in present-day OTFT technology. A first challenge is created by the fact that in common OTFT technologies only unipolar, organic semiconductors are available. In our case, the design of the organic RFID transponder chip was limited to p-type only logic, since pentacene is a hole transport semiconductor. In addition, only a single threshold voltage is present in this technology. As a consequence of this, designs based on complementary logic or dual-threshold voltage logic (e.g. nMOS) cannot be implemented. Therefore, in the field of organic electronics, research towards complementary logic has gained considerable attention, potentially leading to an improvement of the robustness of organic circuitry. Very recently, the first 4-bit complementary organic RFID tag has been demonstrated (Blache et al., 2009).

A big challenge in designing complex organic circuitry is the intrinsic parameter spread, in particular on the threshold voltage and the mobility (De Vusser et al., 2006). To tackle this problem in the design, we used a Monte Carlo tool to distribute the transistor parameters randomly for each OTFT in the circuit and to vary these parameters randomly for every new simulation according to the nominal value and within the given spread values for each parameter. The outcome of multiple simulations provides an idea of the robustness of the design and allows to investigate design improvements for increased robustness. To allow such statistical design, the number of transistors in the organic RFID transponder chip has been kept very limited.

Possible gate design architectures in unipolar, single threshold voltage logic are depletion-mode logic or enhancement-mode logic (Cantatore et al., 2007). The gates in our organic RFID transponder chip are designed using the former, which is also known as zerovgs-logic. The choice for this type of logic was driven by the fact that the OTFTs used in this work show normally-on or depletion-mode behavior. The final design of the organic transponder chip has been made using only inverters and NAND-gates, both implemented in the zerovgs-logic as depicted in Fig. 4. The gain of such an inverter at the trip point, for supply voltages of 10 and 20 V, is 1.75 and 2.25, respectively. Nineteen-stage ring oscillators of inverters operate at a frequency of 627 Hz using 10 V supply voltage and at 692 Hz using 20 V supply voltage.
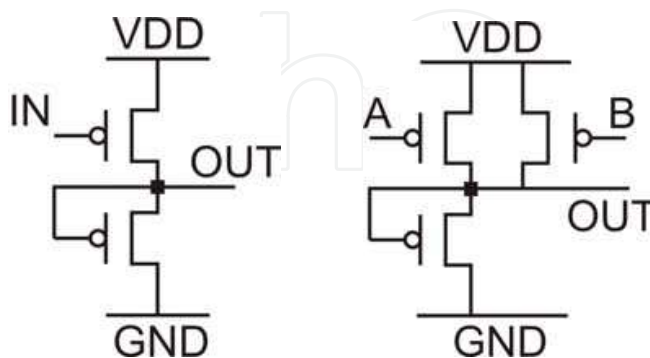

Fig. 4. p-type only inverter (left) and NAND-gate (right) using the zerovgs-logic.

3.2 Final design of the transponder chip

The schematic of the transponder foil is depicted in Fig. 5. A 19-stage ring oscillator generates the clock signal when powered. This clock signal is used to clock the output

register, the 3-bit binary counter and the 8-bit line select. The 8-bit line select has an internal 3-bit binary counter and a 3-to-8 decoder. This block selects a row of 8 bits in the code. The 3-bit binary counter drives the 8:1 multiplexer, selecting a column of 8 bits in the code matrix. The data bit at the crossing of the active row and column, is transported via a 8:1 multiplexer to the output register, which sends this bit on the rising edge of the clock to the modulation transistor. The 3 bits of the 3-bit binary counter are also used in the 8-bit line select block for selecting a new row after all 8 bits in a row are transmitted.
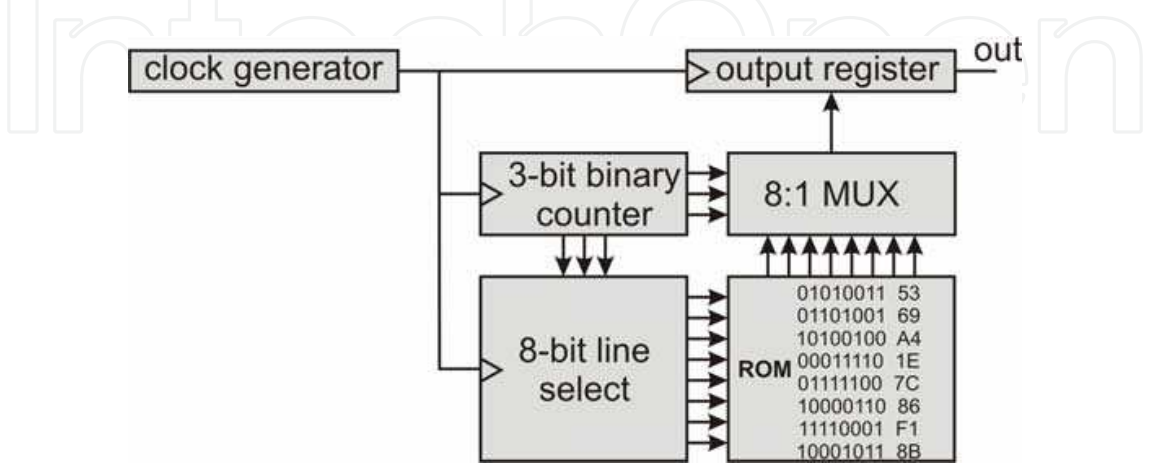
Fig. 5. Schematic overview of the digital logic part of the 64-bit transponder chip.

The 64-bit transponder foil comprises only 414 OTFTs. Figure 2 shows a micrograph image of the transponder foil. At 14 V supply voltage the 64-bit transponder foil generates the correct code at a data rate of 752 b/s, which is depicted in Fig. 6. Besides the 64-bit transponder foil, we also designed an 8-bit transponder foil. The main difference in the design is the complexity of the line select.
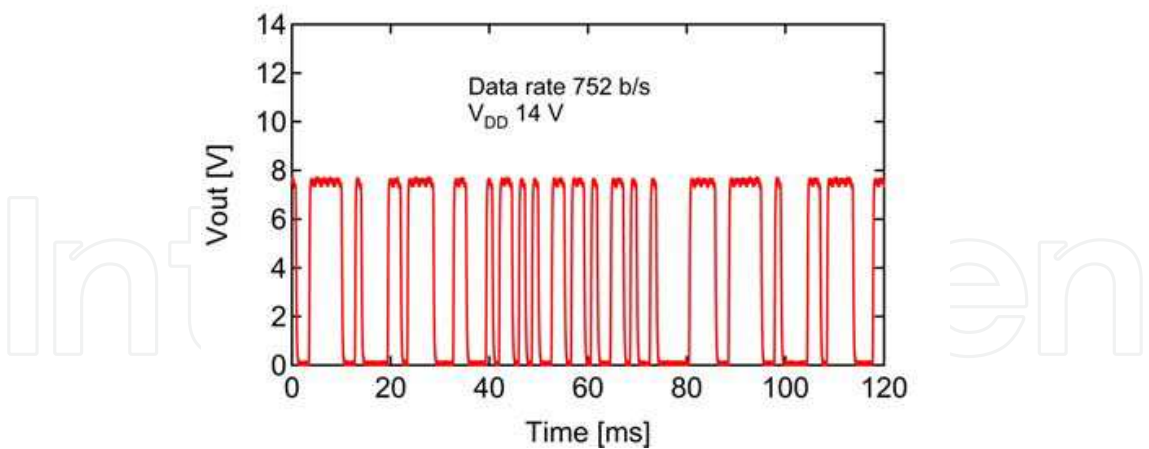

Fig. 6. Measured code of the 64-bit transponder chip at a supply voltage of 14 V.

4. Organic rectifier

4.1 Organic diode

The purpose of the rectifier in an RFID tag is to create a DC-voltage from the AC-voltage detected and generated by an antenna at the targeted base carrier frequency of 13.56 MHz. This frequency is selected because it is a standard in Si-based RFID tags, and will therefore

enable partial compatibility with installed reader systems at 13.56 MHz. An important issue for organic RFID tags is the efficiency of the rectifier. A more efficient rectification will result in the required DC-voltage from lower AC-input voltage. This implies larger reading distances for the RFID tags (Myny et al., 2008; Myny et al., 2009).

A rectifier comprises diodes and capacitors. For organic diodes, two different topologies can be used, being a vertical Schottky diode (Steudel et al., 2005; Pal et al., 2008) and a transistor with its gate shorted to its drain. The transistor with shorted gate-drain node is often considered as the most favorable topology because its process flow is equal to that used for the transistors in the digital circuit of the RFID tag. In this work, however, we have chosen to use the vertical diode structure because of its better intrinsic performance at higher frequencies compared to transistors as diodes (Steudel et al., 2006).

The structure of a vertical, organic diode used to make the rectifier, is drawn in Fig. 7. As depicted, we fabricated hole-only organic diodes with a layer of pentacene (as organic semiconductor) sandwhiched between an Au- and Al-electrode on a 150 mm PEN foil. Because of their workfunctions, the Al-electrode blocks the injection of holes, whereas the Au-electrode permits the injection of holes.
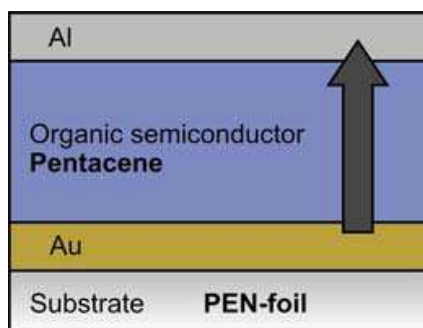

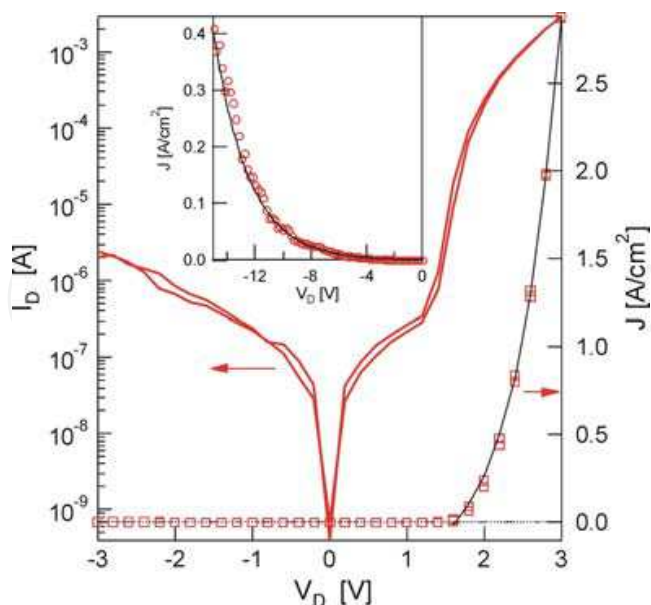Fig. 7. Structure of a vertical, organic Schottky diode.

Fig. 8. $|I|$-V and J-V characteristics of an organic pentacene diode (area=500x200 µm²) on linear (right axis) and logarithmic (left axis) scale. The inset shows the diode leakage current density between 0 and -15 V. The fits to the data of the current densities, both in forward and in reverse biases are represented by the solid black lines.

The electrical behavior of a single organic diode is examined by measurements performed in a nitrogen-filled glove box using an Agilent 4156C parameter analyzer. The current-voltage characteristics of a single pentacene diode are depicted in Fig. 8. The onset voltage of the diode is at about 1.2 V. However, 2 V is required to obtain a current density beyond 200 mA/cm². At 3 V forward bias, the current density is 2.88 A/cm². The leakage current of the diode shows an important increase when the reverse bias increases, limiting the maximum reverse voltage over the diode.

4.2 Organic double half-wave rectifier

A double half-wave rectifier comprises two diodes, each followed by a capacitor (Myny, 2008). Fig. 9a shows the schematic of this circuit. Both capacitors are 20 pF. The active area of the diodes is 500 μm x 200 μm.
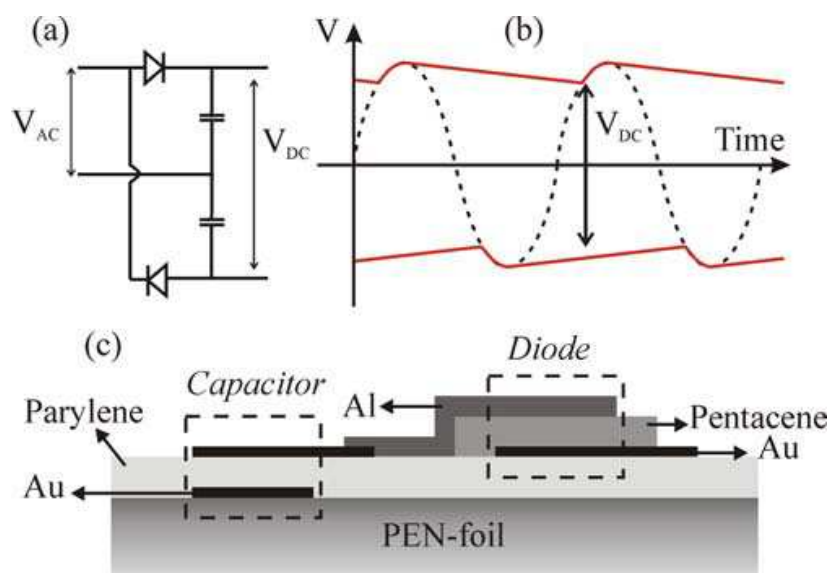
Fig. 9. (a) Schematic of a double half-wave rectifier, (b) schematic operation of a double half-wave rectifier, (c) vertical cross-section of the integrated capacitors and diodes on foil.

A double half-wave rectifier circuit consists of two single half-wave rectifiers connected between the same nodes, with diodes connected as shown in Fig. 9a. Both single half-wave rectifiers rectify the AC input voltage: one rectifies the upper cycles of the AC input voltage, the other single half-wave rectifier rectifies the lower cycles of the input voltage. This is schematically depicted in Fig. 9b. The power and the ground voltage for the digital logic of the RFID tag are taken between both rectified signals (Fig. 9a and b). Therefore, a double half-wave rectifier yields about double the rectified voltage compared to a single half-wave rectifier.

For AC measurements of the rectifiers, we constructed a small printed circuit board (PCB), comprising coax-connections for the AC input signal and the DC output signal. The AC signal is terminated with 50 Ω for limiting reflections at 13.56 MHz. The DC signal is sent to the oscilloscope (MSO6014A of Agilent Technologies) on which the DC voltage was read out, having an input impedance of 1 MΩ, which is the load of the rectifier. The rectifier foil is placed into a socket which is plugged in the PCB. We used a Si-based double half-wave rectifier circuit (assembly of 1N4148-diodes and 20 pF capacitors) as a reference. Fig. 10 plots the rectified DC voltage of the integrated organic and assembled Si-based rectifiers versus

the AC input voltage at a frequency of 13.56 MHz. At an amplitude of the AC voltage of 10.9 V, the rectified DC voltage of the organic rectifier is 14.9 V, while the Si-based rectifier produces 20.6 V. The slope of the measured V_{DCout} as a function of applied V_{ACin}, which we term the efficiency of the rectifier, is 1.64 for the organic rectifiers and 2 for the silicon rectifier. The onset voltage of the diodes can be estimated by extrapolation to an output voltage of 0 V and is 1.98 V for the organic rectifier and 0.42 V for the silicon rectifier. Each organic diode, therefore, has an onset voltage of only about 1 V.
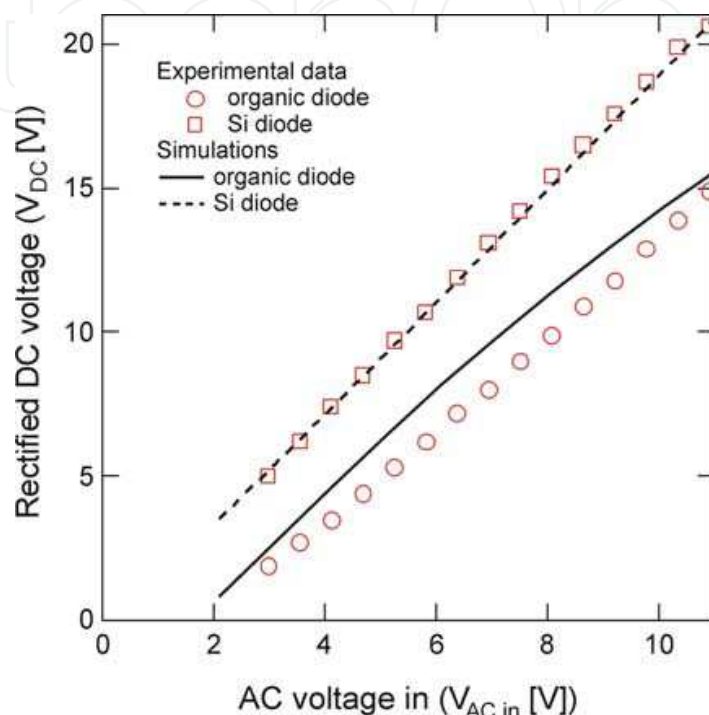

Fig. 10. Simulation results and experimentally obtained data points of the rectified DC output voltage versus the AC input voltage for an organic-based rectifier and a Si-based rectifier both in double half-wave rectifier configuration.

To get a better understanding of the efficiency limitations of the organic-based rectifier, in particular the slope efficiency of V_{DCout}/V_{ACin} = 1.64, we model the behavior of the circuit of Fig. 9 using the characteristics of Fig. 8. Both the forward and the reverse current density J can be expressed quite accurately as a function of the voltage V using the exponential curve $J(V) = J_0 + J_1 \exp(\alpha V)$. In the relevant forward current range (1.6 V to 3 V, see Fig. 8), $J_0 = -0.311$ A/cm², $J_1 = 0.0189$ A/cm² and $\alpha = 1.71$ V⁻¹. In the relevant reverse current range (-15 V to -1 V, see inset Fig. 8), $J_0 = 0$ A/cm², $J_1 = 0.001$ A/cm² and $\alpha = -0.4$ V⁻¹. These fits, extracted from the quasi-static characteristics, have been used to calculate the output voltage (V_{DC}) as a function of the AC input amplitude (V_{in}) by numerically matching the charging and discharging current of the rectifier's capacitors using Eq. (1), derived from the equations and conditions outlined in Steudel et al. (Steudel et al., 2005):

$$\frac{1}{2\pi} \int_{\pi-\sin^{-1}\left(\frac{V_{DC}}{2V_{in}}\right)}^{2\pi+\sin^{-1}\left(\frac{V_{DC}}{2V_{in}}\right)} J\left(V_{in}\sin(\theta)-\frac{V_{DC}}{2}\right)\partial\theta + \frac{V_{DC}}{2AR_L} = \frac{1}{2\pi} \int_{\sin^{-1}\left(\frac{V_{DC}}{2V_{in}}+\frac{1.6}{V_{in}}\right)}^{\pi-\sin^{-1}\left(\frac{V_{DC}}{2V_{in}}+\frac{1.6}{V_{in}}\right)} J\left(V_{in}\sin(\theta)-\frac{V_{DC}}{2}\right)\partial\theta \quad (1)$$

with A being the device area (0.001 cm^2) and R_L being the load resistance (1 MΩ).

For the commercial silicon diode, the curves from the datasheet have been used.

Fig. 10 compares the calculated output voltage with the measured voltage. The slope efficiency is almost exactly reproduced. We can now trace back the origin of the slope efficiency to the presence of the reverse leakage current of the organic diodes: at higher input voltages, the leakage current increases exponentially, which discharges the capacitors, resulting in a lower DC output voltage. On the other hand, the modeled curve overestimates the DC output voltage by approximately a constant amount of 1 V, or 0.5 V for each diode. This has not been elucidated at present, and could be attributed to several factors, for example a slightly higher offset voltage or a slightly degraded mobility of the charge carriers by bias stress during the prolonged measurement time. We conclude from this analysis that the efficiency of the rectifier depends on the on/off ratio of the diode current.

5. Organic RFID tag using DC load modulation

In this part, the organic RFID transponder foils are integrated with the antenna coil, the HF-capacitor and the rectifier to form an organic RFID tag. In DC load modulation mode, the modulation transistor (W/L = 5040μm/5μm) is placed behind the rectifier, as can be seen in Fig. 1. All foils are placed into a socket and connected as depicted in Fig. 3. The RFID reader is a 7.5 cm radius antenna which emits the field at a base carrier frequency of 13.56 MHz. In Fig. 11, the internal rectified voltage of this double half-wave rectifier in the organic RFID tag is plotted as a function of the field generated by the reader, for the tag antenna placed in the near-field of the reader antenna, at a distance of about 4 cm from the coil generating the readers 13.56 MHz RF field. As can be seen in the graph, 10 V rectified voltage is obtained at a 13.56 MHz electromagnetic field of about 0.9 A/m, and 14 V at 1.26 A/m. The latter is the voltage currently required by our 64-bit organic transponder chips. The ISO 14443 standard states that RFID tags should be operational at a minimum required RF magnetic field strength of 1.5 A/m. The double half-wave rectifier circuit presented here therefore satisfies this ISO norm. After extrapolation of the measurement data, a DC voltage of 17.4 V can be obtained at a field of 1.5 A/m. If a single half-wave rectifier was used, the rectified voltage would be limited to 8 - 9 V, which is too low for current organic technology.
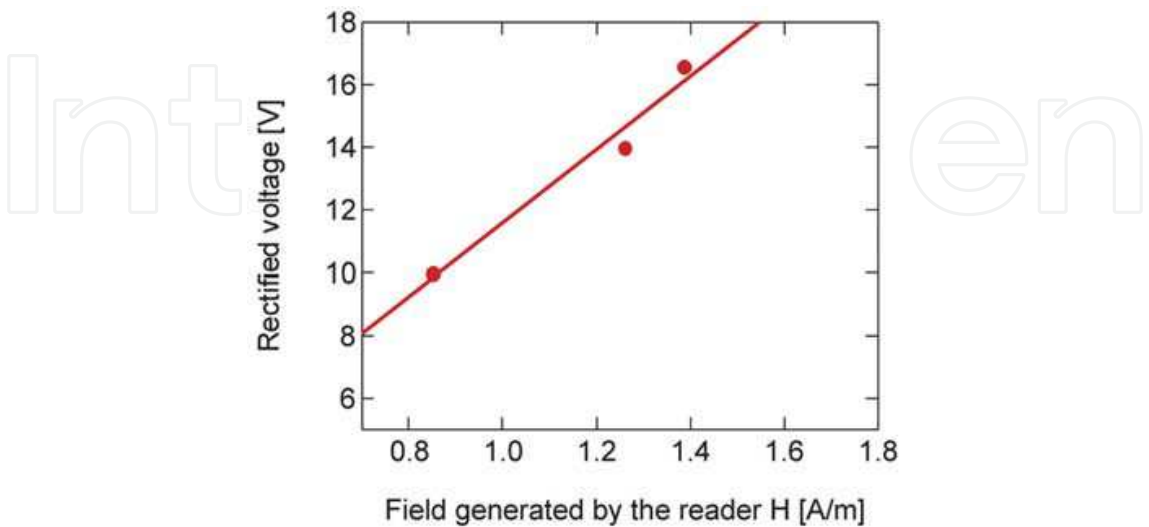

Fig. 11. Internal rectified voltage of a double half-wave rectifier generated in an organic RFID tag versus the 13.56 MHz magnetic field generated by the reader.

The obtained rectified 14 V drives the transponder chip, which sends the code to the modulation transistor. The signal sent from the fully integrated, plastic tag is received by the reader and subsequently visualized using a simple envelope detector (see inset Fig. 12) without amplification. The signal measured at the reader side is depicted in Fig. 12. This shows the fully functional, 64-bit RFID tag using an inductively-coupled 13.56 MHz RFID configuration with a data rate of 787 b/s. With a 0.7 V drop over the diode at the reader (envelope detector), a tag-generated signal of about 1.1 V is obtained, from which 30 mV is load modulation (modulation depth h = 1.4%).
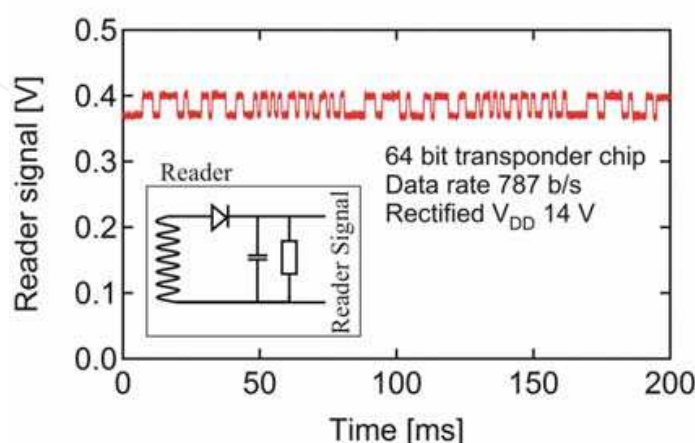

Fig. 12. Signal of the 64-bit RFID tag measured on the reader (unamplified reader signal). The envelope detector of the reader is depicted in the inset.

Two of the reader standards at 13.56 MHz base carrier frequency are the proximity (ISO 14443) and vicinity readers (ISO 15693). The main difference between them is the coil radius, being 7.5 cm for the proximity reader and 55 cm for the vicinity reader. This results in a maximum readout distance of 10 cm for the proximity and 1 m for the vicinity reader. As mentioned earlier, the standard (ISO 14443) states also that the tag should be operational at an RF magnetic field of 1.5 A/m, which is significantly lower than the maximum allowed RF magnetic field of 7.5 A/m. One can calculate the required magnetic field at the antenna centre in order to obtain the required field to operate the tag. In our case, the required field for an 8-bit organic RFID tag was 0.97 A/m. This is depicted in Fig. 13. The dots in this graph show the experimental data at distances of 3.75, 8.75 and 13.75 cm with respect to the field generating antenna. This graph shows that it is possible to energize the 8-bit organic RFID tag at maximum readout distances for proximity readers below the maximum allowed RF magnetic field. The signal detected by the reader during the same experiment is depicted in Fig. 14 at distances of 5 and 10 cm with respect to the sense coil.

6. Summary

In this chapter, we presented the technology, designs and implementation of an inductively-coupled passive 64-bit organic RFID tag which is fully functional at a 13.56 MHz magnetic field strength of 1.26 A/m. This RF magnetic field strength is below the minimum required RF magnetic field stated in the ISO standards. The 64-bit transponder chip employs 414 OTFTs. It is internally driven by a supply voltage of 14 V generated by an efficient organic, double half-wave rectifier. The obtained data rate of the organic RFID tag is 787 b/s. Also an 8-bit transponder chip was measured in DC load modulation configuration and could be readout at a distance of 10 cm, which is the expected readout distance for proximity readers.
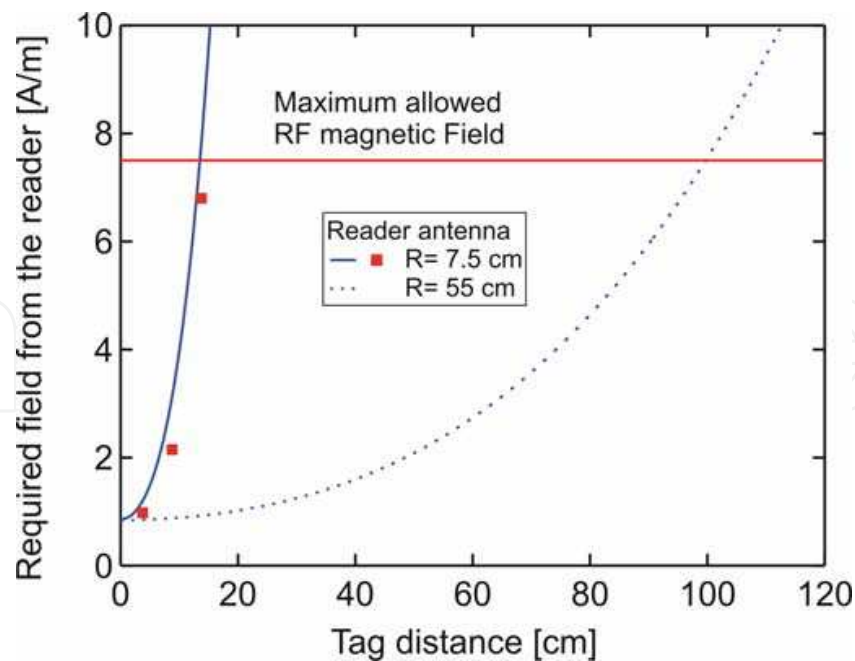
Fig. 13. Calculation and experimentally obtained data of the required RF magnetic field at the reader side as a function of the tag distance in order to generate the required RF magnetic field to operate the tag.
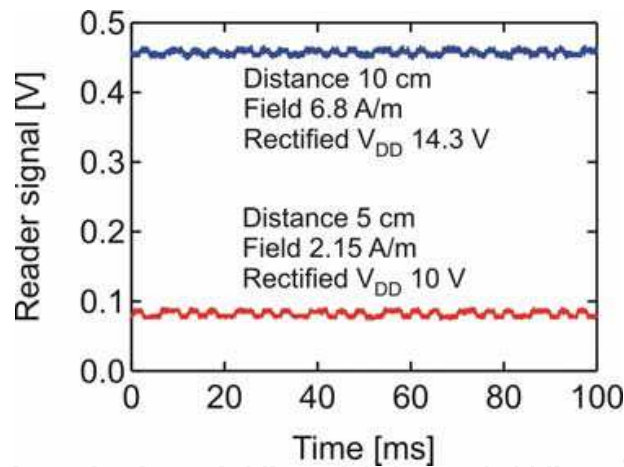

Fig. 14. Signal of the 8-bit RFID tag measured on the reader (unamplified reader signal) in DC load modulation mode at distances of 5 and 10 cm.

7. Future outlook

This work demonstrates that when taking proper care of the critical timing path in digital circuits to account for variability of parameters, state-of-the-art organic electronics technology allows fairly complex digital circuits. Furthermore, the performance of high-frequency analog front-end devices such as rectifiers and load modulators are sufficient for a full organic-based tag to match ISO standards in terms of allowed magnetic field and read-out distance.

A targeted application for organic HF tags is Electronic Product Coding (EPC). Some EPC specifications have already been met by organic tags in recent years, namely the

transmission of a 64 bit or larger code (Cantatore et al., 2007; Ullman et al., 2007; Myny et al., 2009), the compatibility with regulations concerning human exposure to electromagnetic fields (Myny et al., 2009). Furthermore, EPC prescribes Manchester encoding of the data, several types of memory (i.e. write-once-read-many) and a basic anti-collision protocol. These have all been shown to date (Myny et al., 2009). Nevertheless, state-of-the-art organic transponder chips fall short of complying with other EPC specifications. Significantly higher data rates (26.48kb/s to 52.969kb/s) are needed as compared to the hundreds b/s up to 2000 b/s of the state-of-the-art organic RFID tags (Cantatore et al., 2007; Ullman et al., 2007; Myny et al., 2009). Furthermore, EPC specifications require a data clock on the tag which is derived from and synchronous with the RF carrier wave. Furthermore, the communication between reader and tag has to be bi-directional, in particular to implement anti-collision protocols where the reader talks first. All latter requirements are currently in research stage, but not demonstrated yet with organic electronics.

8. Acknowledgements

9. References

Blache, R.; Krumm, J. & Fix, W. (2009). Organic CMOS Circuits for RFID Applications, *IEEE International Solid-State Circuits Conference Digest Technical Papers*, pp. 208-9, USA, 2009, San Francisco

Cantatore, E.; Geuns, T. C.T.; Gelinck, G. H.; van Veenendaal, E.; Gruijthuijsen, A. F.A.; Schrijnemakers, L.; Drews, S. & de Leeuw, D. M. (2007). A 13.56-MHz RFID System Based on Organic Transponders, *IEEE Journal of Solid-State Circuits*, 42, 2007, 84-92

De Vusser, S.; Genoe, J. & Heremans, P. (2006). Influence of Transistor Parameters on the Noise Margin of Organic Digital Circuits, *IEEE Transactions on Electron Devices*, 53, 2006, 601-10

Gelinck, G. H.; Huitema, H. E.A.; van Veenendaal, E.; Cantatore, E.; Schrijnemakers, L.; van der Putten, J. B.P.H.; Geuns, T. C.T.; Beenhakkers, M.; Giesbers, J. B.; Huisman, B.-H.; Meijer, E. J.; Benito, E. M.; Touwslager, F. J.; Marsman, A. W.; van Rens, B. J.E. & de Leeuw, D. M. (2004). Flexible active-matrix displays and shift registers based on solution-processed organic transistors, *Nature Materials*, 3, 2004, 106-10

Huitema, H. E.A.; Gelinck, G. H.; van Veenendaal, E.; Cantatore, E.; Touwslager, F. J.; Schrijnemakers, L. R.; van der Putten, J. B.P.H.; Geuns, T. C.T. & Beenhakkers, M. J. (2003). A Flexible QVGA Display With Organic Transistors, *Proceedings of International Display Workshops*, pp. 1663-1664, Japan, 2003, Fukuoka

Myny, K.; Steudel, S.; Vicca, P.; Genoe J. & Heremans, P. (2008). An integrated double half-wave organic Schottky diode rectifier on foil operating at 13.56 MHz, *Applied Physics Letters*, 93, 2008, 093305

Myny, K.; Steudel, S.; Vicca, P.; Beenhakkers, M. J.; van Aerle, N. A.J.M.; Gelinck, G. H.; Genoe, J.; Dehaene, W. & Heremans, P. (2009). Plastic circuits and tags for HF radio-frequency communication, *Solid-State Electronics,* 53, 2009, 1220-1226

Pal, B. N.; Sun, J.; Jung, B. J.; Choi, E.; Andreou, A. G. & Katz, H. E. (2008). Pentacene-Zinc Oxide Verical Diode with Compatible Grains and 15-MHz Rectification, *Advanced Materials*, 20, 2008, 1023-1028

Steudel, S.; Myny, K.; Arkhipov, V.; Deibel, C.; De Vusser, S.; Genoe, J. & Heremans, P. (2005). 50 MHz rectifier based on an organic diode, *Nature Materials*, 4, 2005, 597-600

Steudel, S.; De Vusser, S.; Myny, K.; Lenes, M.; Genoe, J. & Heremans, P. (2006). Comparison of organic diode structures regarding high-frequency rectification behavior in radio-frequency identification tags, *Journal of Applied Physics*, 99, 2006, 114519

Ullmann, A.; Böhm, M.; Krumm, J. & Fix, W. (2007). Polymer Multi-Bit RFID Transponder, *International Conference on Organic Electronics*, abstract 53, The Netherlands, 2007, Eindhoven
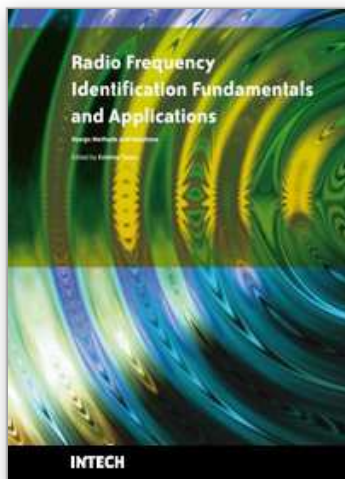
Radio Frequency Identification Fundamentals and Applications Design Methods and Solutions

Edited by Cristina Turcu

This book, entitled Radio Frequency Identification Fundamentals and Applications, Bringing Research to Practice, bridges the gap between theory and practice and brings together a variety of research results and practical solutions in the field of RFID. The book is a rich collection of articles written by people from all over the world: teachers, researchers, engineers, and technical people with strong background in the RFID area. Developed as a source of information on RFID technology, the book addresses a wide audience including designers for RFID systems, researchers, students and anyone who would like to learn about this field. At this point I would like to express my thanks to all scientists who were kind enough to contribute to the success of this project by presenting numerous technical studies and research results. However, we couldn't have published this book without the effort of InTech team. I wish to extend my most sincere gratitude to InTech publishing house for continuing to publish new, interesting and valuable books for all of us.

How to reference

In order to correctly reference this scholarly work, feel free to copy and paste the following:

Kris Myny, Soeren Steudel, Peter Vicca, Monique J. Beenhakkers, Nick A.J.M. van Aerle, Gerwin H. Gelinck, Jan Genoe, Wim Dehaene, and Paul Heremans (2010). Organic RFID Tags, Radio Frequency Identification Fundamentals and Applications Design Methods and Solutions, Cristina Turcu (Ed.), ISBN: 978-953-7619-72-5, InTech, Available from: http://www.intechopen.com/books/radio-frequency-identification-fundamentals-and-applications-design-methods-and-solutions/organic-rfid-tags

INTECH
open science | open minds